Rhodopsin Activation: Effects on the Metarhodopsin I–Metarhodopsin II Equilibrium of Neutralization or Introduction of Charged Amino Acids within Putative Transmembrane Segments†

Charles J. Weitz*,‡,§ and Jeremy Nathans‡,∥

Department of Molecular Biology and Genetics and Department of Neuroscience, The Johns Hopkins University School of Medicine, Baltimore, Maryland 21205, and Howard Hughes Medical Institute, Baltimore, Maryland 21205

Received June 4, 1993; Revised Manuscript Received September 27, 1993®

ABSTRACT: We have studied the metarhodopsin I (M I)–metarhodopsin II (M II) equilibria of expressed wild-type and mutant rhodopsins. We studied two classes of mutants with amino acid substitutions in or near the putative transmembrane segments: those in which a charged residue was replaced by a neutral residue (or in one case another charged residue) and those in which a neutral residue likely (or postulated) to be in proximity to the retinylidene Schiff's base was replaced by a charged residue. In the first class, we found mutants that abnormally favored M II (replacements of Asp-83, Glu-134, or Arg-135) as well as one that abnormally favored M I (replacement of Glu-122). In the second class, we found several mutants that abnormally favored M I, the most extreme being those in which glutamate replaced His-211 or Ala-292. These studies suggest that electrostatic forces play a major role in the energetics of the M 1-to-M II transition, and they indicate that electrostatic perturbation in the vicinity of the protonated retinylidene Schiff's base is a plausible mechanism for the change in its pK_a that is associated with the M I–M II transition. They further suggest that the highly conserved pair of charged residues homologous to Glu-134 and Arg-135 may play a general role in agonist-dependent conformational changes in G-protein-coupled receptors.

Following photoisomerization of 11-*cis*-retinal, rhodopsin passes through a series of photoproducts originally defined by their characteristic absorption spectra (Yoshizawa & Shichida, 1982). This series of photoproducts represents a process of thermal relaxation in which enthalpy stored in the highly-strained configuration of *all-trans*-retinal (Birge et al., 1988; Smith et al., 1991) in early photoproducts is transferred to the protein moiety (opsin) to drive a conformational change.

An extensive body of evidence indicates that a large conformational change in opsin takes place during the M I-to-M II transition and that this structural change is responsible for the generation of the intracellular signal in visual excitation [reviewed in Hofmann (1986)]. The transition of M I to M II is characterized by sensitivity to pH (Mathews et al., 1963), uptake of at least two protons into opsin (Radding & Wald, 1956; Bennett, 1980), deprotonation of the retinylidene Schiff's base, leading to the UV absorbance maximum of M II (Doukas et al., 1978), an increase in the effective volume of the protein (Lamola et al., 1974), and increased accessibility of the cytoplasmic carboxy-terminal tail to proteolytic digestion (Kuhn et al., 1982). Spectroscopic studies of the M I–M II equilibrium revealed that addition of the rod photoreceptor G-protein transducin in the absence of GTP shifts the equilibrium toward M II (Emeis et al., 1982; Bennett et al., 1982) and that addition of GTP abolishes this shift (Emeis et al., 1982). These observations strongly suggest that M II is the photoproduct that specifically binds to transducin and catalyzes GDP–GTP exchange. This conclusion has been further strengthened by kinetic studies, which show a tight correlation between the decay of M II and the decline of the activity catalyzing transducin GDP–GTP exchange (Kibelbek et al., 1991).

Studies of chemically-modified rhodopsin and of expressed mutant rhodopsins have provided insight into the processes that regulate the formation of M II. A rhodopsin derivative in which the retinylidene Schiff's base was methylated, thereby fixing the positive charge on the Schiff's base nitrogen, generated a long-lived M I-like photoproduct and was unable to activate transducin (Longstaff et al., 1986). These observations indicate that deprotonation of the retinylidene Schiff's base is necessary both for the formation of an M II-like photoproduct and for productive coupling to transducin. A mutant opsin in which Glu-113, the counterion for the protonated retinylidene Schiff's base linkage at Lys-296 (Sakmar et al., 1989; Zhukovsky & Oprian, 1989; Nathans, 1990b), was replaced by glutamine formed a visual pigment after incubation with *all-trans*-retinal and activated transducin without exposure to light (Sakmar et al., 1989). Recent observations indicate that mutant opsins substituted at Glu-113 or Lys-296 can activate transducin in the absence of a retinal chromophore (Robinson et al., 1992). These experiments argue that the absence of a positively-charged side chain at position 296 (due either to the absence of the stabilizing counterion or to replacement of Lys-296) is sufficient to drive the protein into an active M II-like conformation. They further suggest that in wild-type rhodopsin a positive charge on the Schiff's base nitrogen at Lys-296 favors an inactive conformation with high affinity for 11-*cis*-retinal and low affinity for *all-trans*-retinal, thus assuring the fidelity of phototransduction. It may also be the case that in the absence of retinal Glu-113 similarly interacts with a protonated ϵ-amino group of Lys-296 (Robinson et al., 1992).

† This work was supported by the Howard Hughes Medical Institute and by the National Eye Institute (National Institutes of Health).

* Address correspondence to this author.

‡ The Johns Hopkins University School of Medicine.

§ Present address: Department of Neurobiology, Harvard Medical School, Boston, MA 02115.

∥ Howard Hughes Medical Institute.

® Abstract published in *Advance ACS Abstracts,* December 1, 1993.

0006-2960/93/0432-14176$04.00/0

Together these results indicate that a key step in the formation of M II is the disruption of the ionic interaction between Glu-113 and the protonated retinylidene Schiff's base. In a recent spectroscopic study of the M I–M II equilibria of expressed mutant rhodopsins, those mutants in which His-211 was replaced by either phenylalanine or cysteine showed an apparent blockade in M I and a loss of pH-sensitivity (Weitz & Nathans, 1992). These data suggest that His-211 is the site where proton uptake is coupled to the formation of M II, as inferred from pH-titration studies of the M I–M II equilibrium (Mathews et al., 1963). On this hypothesis, two general models can relate the importance of His-211 to the formation of M II and the deprotonation of the Schiff's base (Weitz & Nathans, 1992). In the direct model, His-211 is postulated to lie adjacent to the ion pair between Glu-113 and the protonated Schiff's base. Upon protonation, His-211 would lower the pK_a of the Schiff's base by interacting with Glu-113 or Lys-296. The direct model is at odds with models of rhodopsin structure based on analogy with bacteriorhodopsin or with related hormone receptors, which place the fifth transmembrane helix far from the Schiff's base linkage in the seventh transmembrane helix (Oprian, 1992); although it is clearly different from bacteriorhodopsin, the projection structure at 9-Å resolution recently obtained for rhodopsin does not settle this issue, because the identities of the individual transmembrane helices could not be determined (Schertler et al., 1993). In the indirect model, protonated His-211 is postulated to interact not with the ion pair but with some other charged or polar target residue, providing the driving force for a conformational rearrangement that indirectly destabilizes the electrostatic interaction between Glu-113 and the protonated Schiff's base.

To test the role of electrostatic forces in the formation of M II and to test predictions of the direct and indirect models proposed to link protonation of His-211 to the formation of M II, we used site-directed mutagenesis and cDNA expression in human embryonic kidney cells (293s) to prepare mutant bovine rhodopsins for spectroscopic analysis of the M I–M II equilibrium. In the first series of experiments, we studied the effects of neutral substitution of each of the seven charged residues within or adjacent to the transmembrane segments, residues which could plausibly interact with His-211 or electrostatically influence the pK_a of the Schiff's base. In the second series of experiments, we studied the effects of direct electrostatic perturbation on the protonated Schiff's base by introducing charged residues into various positions likely to be in close proximity to the Schiff's base.

MATERIALS AND METHODS

In Vitro Mutagenesis. pCIS-Rho expression plasmids were prepared by oligonucleotide-directed mutagenesis and propagation of the plasmids in *Mut L Escherichia coli*. The opsin coding region was transferred into the parental pCIS vector, and wild-type *E. coli* harboring the mutant plasmid were identified by colony blot hybridization (Nathans, 1990a; Weitz & Nathans, 1992). The entire opsin coding region of each expression plasmid was sequenced on one strand to exclude spurious mutations and to verify the expected one.

Transient Transfection. To generate sufficient rhodopsin for a pair of difference absorption spectra, 20–50 10-cm plates of 293s cells were cotransfected with a mutant pCIS-Rho and pRSV-Tag by the calcium phosphate precipitation method and harvested 48 h later (Nathans, 1990a).

Preparation of Rhodopsin from Expressed Opsin. Membranes were purified from transfected cells by cell homogenization and sucrose density gradient ultracentrifugation, and the membrane fraction was solubilized in digitonin and incubated in the dark with 11-*cis* retinal (Weitz & Nathans, 1992). Bovine rod outer segment (ROS) rhodopsin was prepared as described by Papermaster and Dreyer (1974).

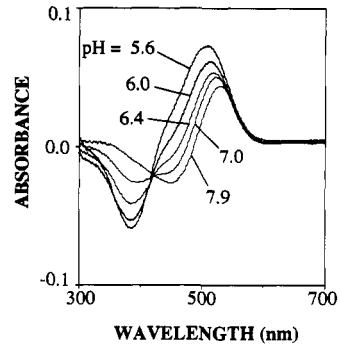

FIGURE 1: Example of control absorption difference spectra of the M I–M II equilibrium from ROS rhodopsin at five different pH values. In combination with estimations of M I and M II from standard absorption spectra [as described in Mathews et al. (1963)], λ_{max} estimates from ROS difference spectra were used to derive the empirical formula for determining the log $K_{eq,app}$ of expressed wild-type and mutant rhodopsins from their difference spectra (see Materials and Methods and Table 1).

UV–Visible Absorption Spectroscopy and Calculation of Difference Spectra. Preparation of samples, photobleaching absorption difference spectra, and M I–M II equilibrium absorption difference spectra were performed as described (Weitz & Nathans, 1992). Briefly, samples of expressed rhodopsin (0.5–1.0 mL) solubilized in digitonin (2.3–3.0%, depending on the anticipated dilution from reagents yet to be added) were divided into two or three aliquots, and the aliquots were adjusted to the appropriate pH by addition of 1 M sodium phosphate (pH 5.6 or 7.9); for experiments using sodium cholate, samples were adjusted to the indicated final concentration by addition of the appropriate volume of a 20% stock solution. All samples had a final sodium phosphate concentration of 150 mM and a digitonin concentration of 2%. Measured pH values were within ±0.1 pH unit of 5.8 or 7.8, as stated, and the measured temperature of all samples was within 1.5–2.5 °C. Photoirradiation was performed (5 min) with a 150-W source attached to a fiberoptic guide. The light beam passed through a 580-nm narrow band-pass filter mounted approximately 5 mm above the cuvette. Under these conditions, no changes in spectra were detected with longer irradiation times, indicating that photo-steady-state was achieved. For all difference spectra, the average of four successive postirradiation spectra was subtracted from the average of four successive preirradiation spectra.

Determination of the Apprent Equilibrium Constant ($K_{eq,app}$) from Difference Spectra. In a series of control experiments, the K_{eq} values of M I–M II equilibria (K_{eq} = [M II]/[M I]) from ROS rhodopsin solubilized in 2% digitonin at pH 5.6, 6.0, 6.4, 7.0, and 7.9 were derived from absorption spectra after subtracting the absorption due to photoregenerated rhodopsin and isorhodopsin (Mathews et al., 1963). Difference spectra were then calculated from the pre- and postirradiation absorption spectra, and, as was shown previously (Weitz & Nathans, 1992), a consistent relationship between the λ_{max} in the difference spectrum and the value of the M I–M II equilibrium is apparent (one set of such difference spectra is shown in Figure 1). We utilized this relationship to develop an empirical method to compare equilibria of expressed wild-type and mutant rhodopsins, which for technical reasons cannot readily be produced in the

Table 1: Relationship of the M I–M II Equilibrium Constant Measured from Standard Absorption Spectra ($K_{eq,estimated}$) to the Wavelength of Maximum Absorption (λ_{max}) in M I–M II Difference Spectra from ROS Rhodopsin Solubilized in 2% Digitonin[a]

pH	mean log K_{eq}	mean λ_{max} ± SEM (nm)	experiments (N)
5.6	0.58	510 ± 1.0	4
6.0	0.33	514 ± 1.5	3
6.4	0.01	518 ± 1.0	3
7.0	−0.33	524 ± 0.3	3
7.9	−0.80	526 ± 0.6	5

[a] This empirical relationship was used to derive the equation for determining the apparent equilibrium constant ($K_{eq,app}$) of M I–M II equilibria of expressed rhodopsins from their M I–M II difference spectra (see Materials and Methods and Figure 1).

quantities typically used for standard M I–M II measurements of ROS rhodopsin. First we obtained an accurate determination of the wavelength of maximum absorption (λ_{max}) from the ROS M I–M II difference spectra by calculating the best-fitting fifth-order polynomial for a small region of the spectrum centered about the maximum using a MacIntosh IIci equipped with Cricket Graph software (Table 1). Next these λ_{max} values were plotted as a function of the K_{eq} values determined from the original control spectra, and the best-fitting equation relating these two variables was calculated (Cricket Graph). This equation is $\log x = (518 - y)/12.1$, where $x = K_{eq,app}$ and $y = \lambda_{max}$ in nanometers ($R^2 = 0.96$; $P < 0.05$). From this equation, we have derived the $K_{eq,app}$ values from the M I–M II difference spectra of expressed rhodopsins. It is important to note that this empirical method for determination of $K_{eq,app}$ for expressed mutant rhodopsins rests on the assumptions that the mutants follow the classical photointermediate decay pathway and that the molar extinction coefficients and absorption spectra of the mutant M I and M II photoproducts are not altered by the mutations. (The ground-state spectra are not significantly altered; see below.) If for any mutant one or both of these assumptions is false, then the $K_{eq,app}$ value will be invalid.

The apparent free energy change (ΔG_{app}) was calculated from the $K_{eq,app}$ values from the equation $\Delta G = -2.3RT \log K_{eq}$, where R is the gas constant and T is the absolute temperature (275 K for the samples).

RESULTS

Measurements of M I–M II Equilibria of Expressed Rhodopsins. Following photoexcitation at temperatures near 0 °C, the decay of M II is sufficiently slow that the M I–M II equilibrium is stable for many minutes, permitting the use of conventional spectroscopy to characterize the equilibrium (Mathews et al., 1963). We have used a difference spectroscopy method to monitor the M I–M II equilibrium from expressed rhodopsins because it provides a high signal-to-noise ratio and is insensitive to photostable contaminants present in the preparations. With this assay, a characteristic family of curves is obtained, each member corresponding to a different value of the equilibrium (Weitz & Nathans, 1992). The difference spectrum reflects the absorption spectrum of rhodopsin (λ_{max} = 498 nm) minus the absorption spectrum of the photoproducts at equilibrium. In the theoretical case where all of the rhodopsin is converted to M I (λ_{max} = 478 nm) and neglecting the fraction of total rhodopsin that is present as photoregenerated rhodopsin at photo-steady-state, the difference spectrum would show a small-amplitude positive peak (due to the large overlap between rhodopsin and M I) with λ_{max} = 538 nm (the point on the long-wavelength limb of the rhodopsin spectrum that is maximally greater in absorbance than the M I spectrum), and a nearly-symmetric negative peak centered at 458 nm (the point on the short-wavelength limb of the M I spectrum that is maximally greater in absorbance than the rhodopsin spectrum). These values were calculated on the assumption that rhodopsin and M I have essentially the same molar extinction coefficients (Mathews et al., 1963) and that the waveforms of their absorption spectra are the same. Under conditions where the equilibrium is progressively shifted toward M II, the amplitude of the M I spectrum becomes progressively smaller in comparison with the amplitude of the preirradiation rhodopsin spectrum, and the positive difference peak therefore grows progressively larger in amplitude and its λ_{max} moves toward shorter wavelengths until it reaches a limit of 498 nm, corresponding to the theoretical case in which all of the rhodopsin has been converted to M II (λ_{max} = 380 nm). The M II spectrum appears in the difference spectrum as a negative peak that does not significantly overlap with the spectrum of rhodopsin.

Control experiments with bovine rod outer segment (ROS) rhodopsin studied at a range of pH values show that the value of the apparent K_{eq} for the M I–M II equilibrium can be estimated from a difference spectrum (see Materials and Methods, above; Figure 1 and Table 1). The estimate of $K_{eq,app}$ from this method is most accurate when the λ_{max} of the positive peak in the difference spectrum lies in the central region of its range, which we have set arbitrarily as between 503 and 533 nm, corresponding respectively to log $K_{eq,app}$ values of 1.3 and −1.3. Outside of this region the estimate is likely to be in considerable error because, as discussed above, the λ_{max} values approach a limit at either extreme (498 and 538 nm), a fact not reflected in the equation relating log $K_{eq,app}$ to λ_{max}.

Figure 2 shows the absorption difference spectra of M I–M II equilibria (2 °C) obtained from ROS rhodopsin, expressed wild-type rhodopsin, and 10 mutant rhodopsins at pH 5.8 and 7.8. We have studied the equilibria at two different pH values in order to assess each mutant under conditions where wild-type rhodopsin shows different values of the equilibrium as well as to detect any specific alterations in sensitivity to pH. The mean λ_{max} values from difference spectra from two independent experiments for each mutant at each pH are presented at Table 2, and the calculated $K_{eq,app}$ from each difference spectrum is represented in Figure 3. As previously reported, expressed wild-type rhodopsin (WT) exhibits an equilibrium shifted more toward M II at both values of pH than does ROS rhodopsin (Weitz & Nathans, 1992). After preincubation for 24 h in digitonin with membranes from 293s cells, the cell line used for expression, the M I–M II equilibrium obtained with ROS rhodopsin more closely resembles that from expressed wild-type rhodopsin (Figure 2 and 3, ROS + 293) than it does otherwise. Spectra obtained at different times after mixing digitonin-solubilized ROS with 293s membranes suggest that the residual difference reflects incomplete equilibration of ROS rhodopsin with phospholipids from the 293s membranes (unpublished observations). Under these conditions, the mean log $K_{eq,app}$ value estimated for the equilibrium from expressed wild-type rhodopsin is >1.30 at pH 5.8 and 0.52 at pH 7.8 (Figure 3).

Charge Neutralization Mutants. To test the role of electrostatic forces in the formation of M II and to test plausible targets for His-211 as specified by the indirect model, we studied 10 mutants of bovine rhodopsin. In seven mutants, one each of the seven charged residues in or near the putative transmembrane segments was replaced by a neutral residue (Figure 4); three additional mutants had double substitutions

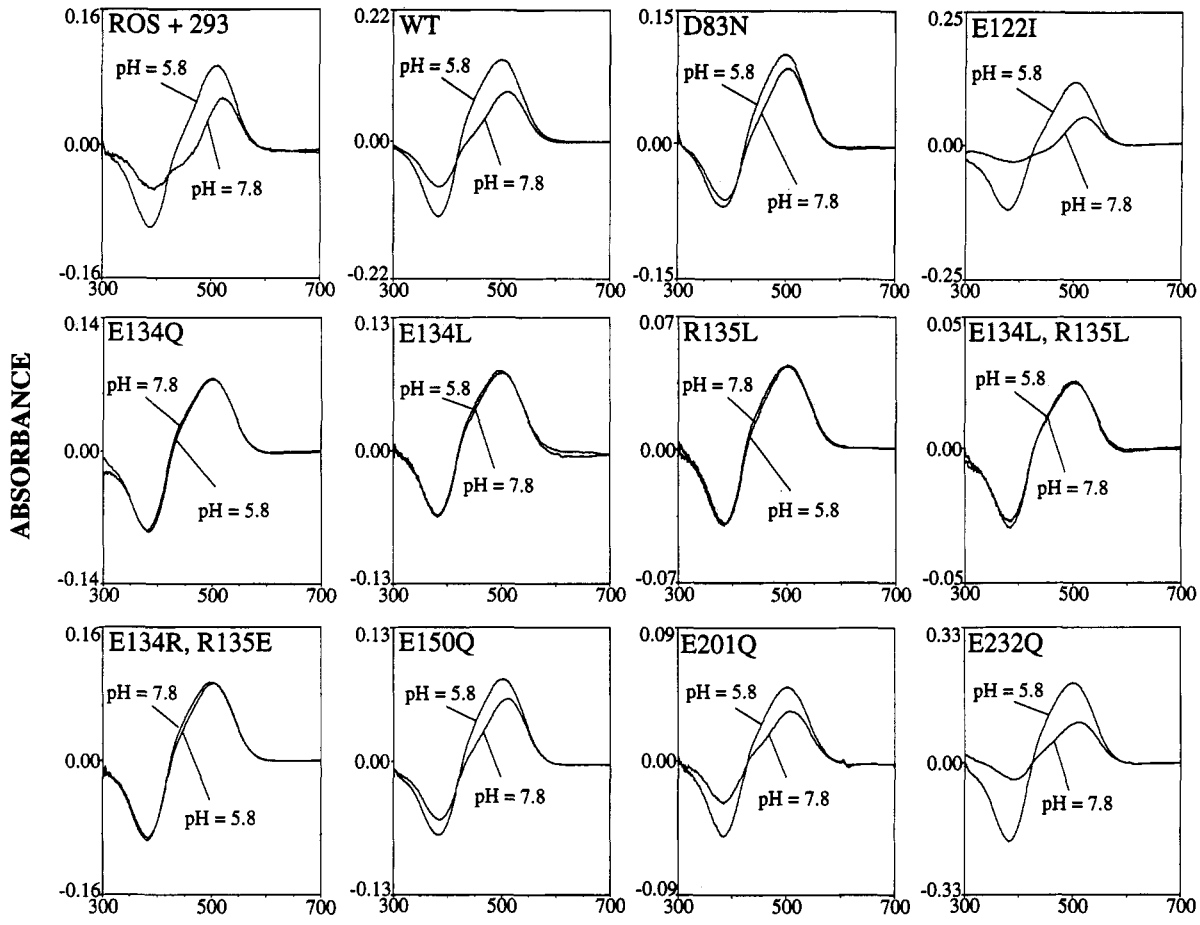

FIGURE 2: Absorption difference spectra showing the effect of pH on the M I–M II equilibrium of wild-type and mutant rhodopsins. ROS + 293: ROS rhodopsin solubilized in digitonin and preincubated for 24 h with membranes from 293s cells, the cell line used for opsin expression. The remaining panels: the M I–M II absorption difference curves of wild-type (WT) and the indicated mutant rhodopsins obtained at pH 5.8 and 7.8. To facilitate comparison, the curves here and in Figures 5 and 8 have been scaled such that the photobleaching difference absorption peak (not shown) would occupy approximately the same fractional area of each panel.

Table 2: Mean λ_{max} Values (nm) of M I–M II Equilibrium Difference Spectra for ROS Rhodopsin and Expressed Wild-Type and Mutant Rhodopsins[a]

rhodopsin	λ_{max}, pH 5.8	λ_{max}, pH 7.8
ROS + 293	504	520
WT	501	512
D83N	499	504
E122I	505	523
E134Q	500	501
E134L	500	499
R135L	501	500
E134L,R135L	502	500
E134R,R135E	502	501
E150Q	501	511
E201Q	503	508
E232Q	502	510
H211E	533	532
A292E	533	534
F293E	507	514
A299E	513	521
V300E	514	530

[a] $n = 2$ for each; calculated log $K_{eq,app}$ values from these experiments are represented in Figure 3.

of Glu-134 and Arg-135, the adjacent pair of charged residues. Each of the mutants has been shown previously to form a visual pigment with ground-state spectroscopic properties not significantly different from wild-type rhodopsin (Nathans, 1990a,b). In general, the substitutions were conservative with respect to size, such as glutamine for glutamate; in the case of Glu-122, we studied E122I because E122Q showed a significant blue-shift in its photobleaching difference spectrum (Nathans, 1990a), a property that would confound the interpretation of the difference spectrum representing the M I–M II equilibrium (Weitz & Nathans, 1992).

Three of the mutants, E150Q, E201Q, and E232Q, differ only minimally from expressed wild-type rhodopsin in the equilibrium at either pH (Figures 2 and 3, Table 2), suggesting that in wild-type rhodopsin these glutamate residues make little contribution to the energetics of the equilibrium or to pH-sensitivity. E122I exhibits a reproducible shift toward M I at both pH points compared with wild-type rhodopsin; the mean difference in ΔG_{app} ($\Delta\Delta G_{app}$, defined as $\Delta G_{mutant} - \Delta G_{wild\text{-}type}$) estimated from the data in Figure 3 is +1.1 kcal/mol at pH 7.8 and $\geq$+0.2 kcal/mol at pH 5.8. This result suggests a contribution of Glu-122 in wild-type rhodopsin to the formation or stabilization of M II.

D83N shows a shift of the equilibrium toward M II at pH 7.8 compared with wild-type (mean log $K_{eq,app} = 1.20$; $\Delta\Delta G_{app} = -0.85$ kcal/mol); this phenotype is nearly identical to that seen in rhodopsin mutant H65F (Weitz & Nathans, 1992). Whether or not a shift toward M II greater than that of wild-type also occurs at pH 5.8 cannot be determined from this

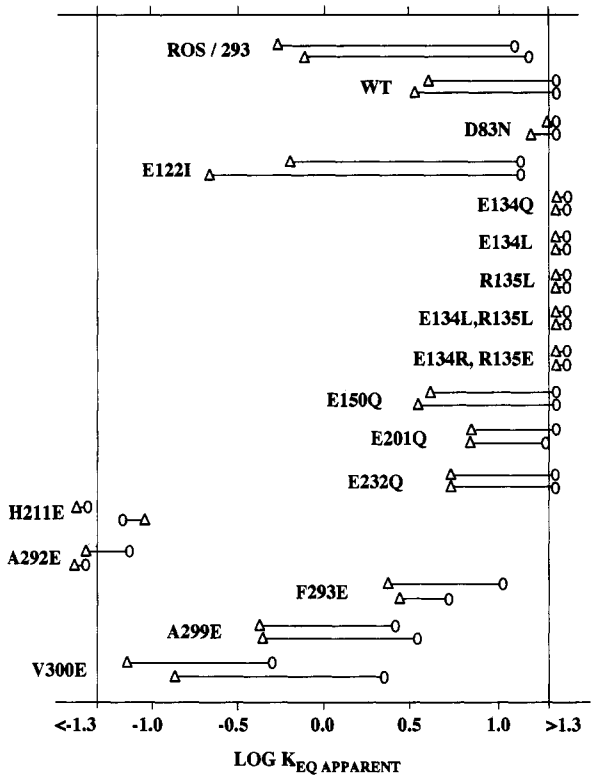

FIGURE 3: Empirically determined log $K_{eq,app}$ of the M I–M II equilibrium for wild-type and mutant rhodopsins at pH 5.8 and 7.8 (see text). For each experiment (in which equilibria at both pH values were assessed), the value of log $K_{eq,app}$ at pH 5.8 is shown by the position of the open circle and that for pH 7.8 by the position of the open triangle; measurements at the two pH values derived from a single experiment are shown as symbols connected by a horizontal line. Two experiments are shown for each visual pigment. For log $K_{eq,app}$ values greater than 1.3 or less than −1.3, the relevant symbol is simply listed in that column. log $K_{eq,app}$ values are shown for H211E and A292E, but these mutants may be kinetically blocked in M I under these conditions (i.e., it is possible that equilibrium was not reached on the time scale of the experiments, as suggested by the photobleaching profile of H211E in Figure 7).

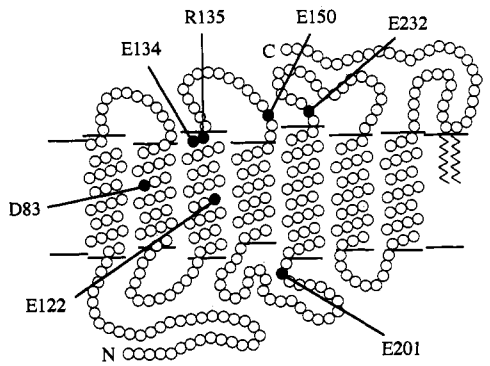

FIGURE 4: Model of the topology of bovine rhodopsin in the ROS disk membrane showing the charged amino acids predicted to lie in or near the transmembrane segments. The C-terminus lies on the cytoplasmic side.

experiment. This result suggests that in wild-type rhodopsin Asp-83 contributes to the stabilization of M I, at least at the alkaline pH.

All five of the mutants with substitutions of Glu-134 or Arg-135 (single mutants E134Q, E134L, and R135L and double mutants E134L,R135L and E134R,R135E) show difference spectra suggestive of a large shift toward M II at both pH 5.8 and pH 7.8 (log $K_{eq,app} > 1.30$ in all cases). Because these difference spectra show no evidence of M I and because the absorption spectrum of released *all-trans*-retinal is similar

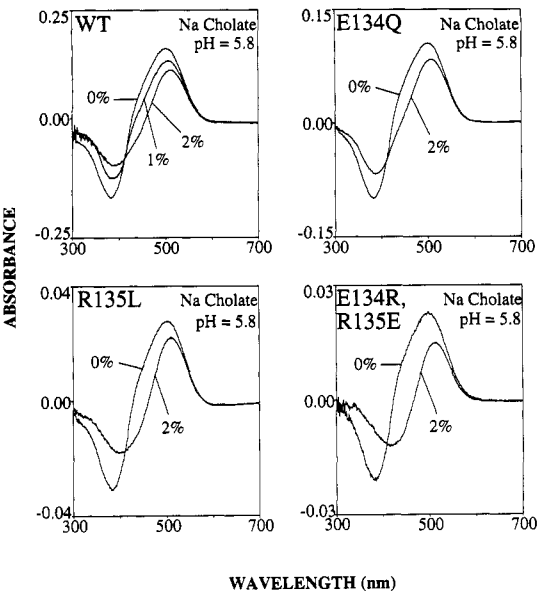

FIGURE 5: Absorption difference spectra showing the effect of sodium cholate on the M I–M II equilibria of wild-type (WT) and mutant rhodopsins. Cholate concentration (w/v) is as indicated for each spectrum.

to that of M II, it was possible that mutants substituted at these positions simply denature rapidly after photoexcitation or exhibit a greatly increased rate of M II hydrolysis, leading to difference spectra difficult to distinguish from those produced by a large shift toward M II. The small differences in molar extinction coefficient and λ_{max} between M II and *all-trans*-retinal often lead to distinguishable difference spectra (Weitz & Nathans, 1992), but these distinguishing features can be obscured by the noise in the UV typical of absorption difference spectra from solubilized membrane preparations (unpublished observations).

To address these possibilities, we reexamined the M I–M II equilibria in the presence of sodium cholate, which has been shown in previous studies to shift the equilibrium toward M I by slowing the forward rate, presumably by altering the physical properties of the lipid or micellar phase (Konig et al., 1989). Figure 5 shows the effect on the M I–M II equilibrium produced by the addition of sodium cholate to the digitonin–membrane micelles in which wild-type rhodopsin (WT), E134Q, R135L, or E134R,R135E had been solubilized. At pH 5.8, expressed wild-type rhodopsin shows a concentration-dependent shift of the equilibrium toward M I. In the presence of 2% cholate, each of the three mutants shows a shift of the equilibrium toward M I that is comparable to that of wild-type (mean log $K_{eq,app}$ values for WT, E134Q, R135L, and E134R,R135E were, respectively, 0.73, 0.81, 0.44, and 0.53; $n = 2$ for each). It is clear that under these conditions E134Q, R135L, and E134R,R135E form M II that is in equilibrium with M I, making unlikely the possibility that the difference spectra in Figure 2 for these mutants reflected denaturation or accelerated Schiff's base hydrolysis. The behavior of the mutants in the presence of cholate at pH 7.8 could not be assessed, since at that pH wild-type rhodopsin fails to show any response to cholate (unpublished observations). Since cholate is largely in its ionized form above pH 6.4, this ineffectiveness could reflect the poor partitioning of ionized cholate into the micelles.

Taken together, these experiments indicate that the mutants in which Glu-134 or Arg-135 is substituted show enhanced formation or stabilization of M II. Compared with wild-type rhodopsin, all five of these mutants favor M II at pH 7.8 by

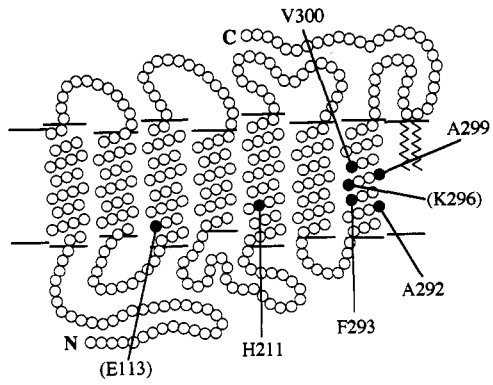

FIGURE 6: Model of the topology of bovine rhodopsin in the ROS disk membrane showing neutral amino acids replaced by charged residues. Also depicted (in parentheses) are Lys-296, the amino acid which forms the retinylidene Schiff's base, and Glu-113, the counterion for the protonated retinylidene Schiff's base.

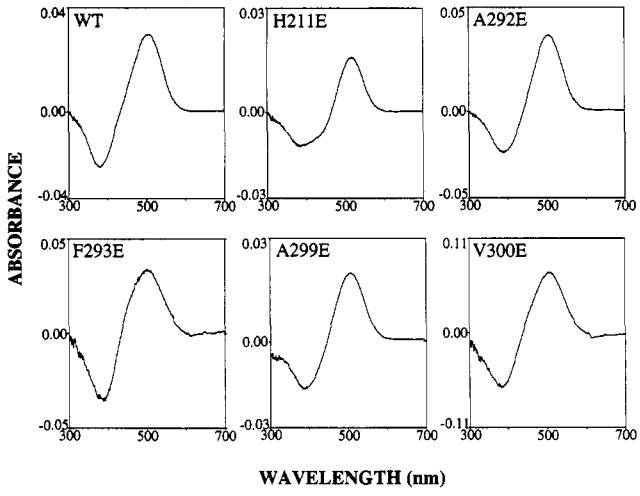

FIGURE 7: Photobleaching difference spectra (25 °C) of expressed rhodopsins solubilized in digitonin.

greater than an estimated additional 0.9 kcal/mol. This phenomenon is true not only of the four mutants in which one or both of the adjacent pair of charged residues is neutralized but also of E134R,R135E, in which the charged residues are exchanged but the overall local charge density is maintained. These observations suggest that in wild-type rhodopsin Glu-134 and Arg-135 make specific electrostatic contacts (to each other or to other residues) that create an energetic barrier to the formation or stabilization of M II.

None of the mutants whose spectra are shown in Figure 2 showed a pH-independent predominance of M I, the phenotype predicted if a target residue with which protonated His-211 interacts has been replaced (Weitz & Nathans, 1992). These results indicate that none of these residues is a unique site with which protonated His-211 interacts to favor M II. These results do not exclude the possibility that some other charged or polar residue could interact with His-211.

Charge Introduction Mutants. To examine the effects on the M I–M II equilibrium of an electrostatic perturbation near the protonated retinylidene Schiff's base, we prepared mutant rhodopsins in which neutral residues expected to be in proximity to Lys-296 were replaced by charged residues (Figure 6). This set included substitutions of residues within the putative seventh transmembrane segment approximately one helical turn below (Ala-292, Phe-293) or above (Ala-299, Val-300) Lys-296 as well as His-211, postulated in the direct model to be situated near Lys-296. Figure 7 shows photobleaching difference spectra (25 °C) for wild-type rhodopsin

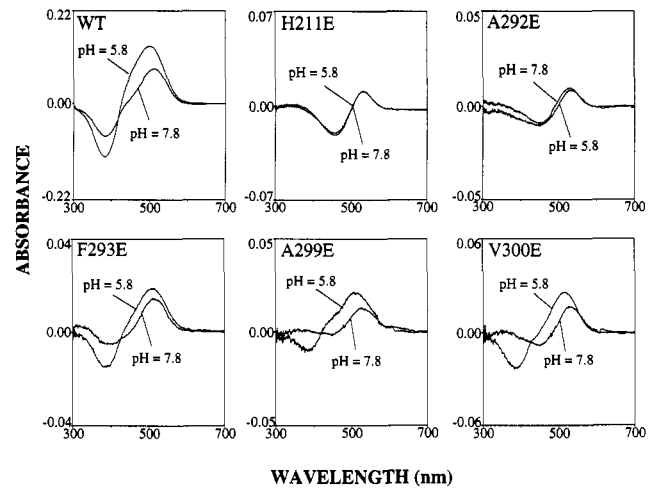

FIGURE 8: Absorption difference spectra showing the effect of pH on the M I–M II equilibrium of wild-type and mutant rhodopsins with charged amino acids replacing neutral ones in positions postulated to be in proximity to the retinylidene Schiff's base (see Figure 2 legend).

(WT) and five mutants, H211E, A292E, F293E, A299E, and V300E. With the exception of H211E, all of the mutants show photobleaching spectra very similar to that of wild-type, indicating that the amino acid substitution in each was tolerated by the protein and had little if any effect on the protein–chromophore interaction in the ground state. Although the ground-state absorption spectrum of H211E is very similar to that of wild-type rhodopsin (unpublished observations), its photobleaching difference spectrum shows a reproducible distortion (Figure 7), suggesting the abnormal persistence of a photoproduct with an M I-like absorption spectrum. Six additional mutants designed to test the effects of positive charge at position 211 or in the vicinity of the Schiff's base, H211K, H211R, A292H, V300H and double mutants E113Q,H211E and E113Q,H211D, failed to generate visual pigments in at least two experiments each (unpublished observations).

Absorption difference spectra of M I–M II equilibria from these mutants are shown in Figure 8. Compared with wild-type rhodopsin (WT), H211E and A292E both show strikingly abnormal spectra, consistent with an essentially complete shift toward M I or kinetic blockade in M I at both pH values. Spectra for each of the other mutants indicate a smaller shift of the equilibrium toward M I, with V300E being shifted most (Figure 3). These experiments indicate that the M I–M II equilibrium is sensitive to electrostatic manipulation of the pK_a of the Schiff's base and argue that the direct model of His-211 action is plausible. They also lend support to the hypothesis that the role played by His-211 in the equilibrium is dependent on its protonation (Weitz & Nathans, 1992), since H211E shows a more severe abnormality than the neutral substitution mutants H211F and H211C—although apparently blocked in M I under standard equilibrium conditions, neither H211F or H211C showed evidence of persistent M I at 25 °C (Weitz & Nathans, 1992).

DISCUSSION

These experiments were performed to examine the contribution of ionizable residues to the energetics of the M I–M II equilibrium and to test predictions of the direct and indirect models of the role of His-211 in Schiff's base deprotonation (see above; Weitz & Nathans, 1992). None of the charge neutralization mutants studied here showed the pH-indepen-

dent predominance of M I predicted of a unique target for His-211 specified in the indirect model, but these findings do not exclude the possibility that some other charged or polar residues could interact with protonated His-211. The effects upon the equilibrium produced by altering the electrostatic environment of the protonated Schiff's base indicate that interaction of the Schiff's base with a charged residue is a plausible mechanism for favoring deprotonation; these results are consistent with either His-211 or some other charged or polar residue playing that role.

The results specifically indicate that in wild-type rhodopsin at least four ionizable residues within the putative transmembrane segments contribute significantly to the energetics of the M I-to-M II transition. Glu-122 contributes to the formation or stabilization of M II, and Asp-83, Glu-134, and Arg-135 act to stabilize M I. These findings make the general point that electrostatic mechanisms play an important role in the transition to M II, consistent with previous work indicating that deprotonation of the Schiff's base is necessary for M II formation (Longstaff et al, 1986). They also indicate that the transition is likely to be regulated by a complex interaction of charged residues with one another and/or with the protonated retinylidene Schiff's base.

Our conclusions that in wild-type rhodopsin Asp-83 and Glu-134 act to favor M I and that Glu-122 acts to favor M II are consistent with previous studies of transducin activation by rhodopsin mutants. Mutants D83N (Nakayama & Khorana, 1991) and E134Q (Sakmar et al., 1989) activate transducin more efficiently than does wild-type rhodopsin, whereas mutants E122Q (Sakmar et al., 1989; Nakayama & Khorana, 1991) and E122A (Nakayama & Khorana, 1991) show a small decrement in transducin activation. Our finding that mutant R135L and double mutants E134L,R135L and E134R,R135E showed a large shift of the equilibrium toward M II (Figures 2 and 3) is superficially at odds with previous studies of transducin activation by expressed rhodopsins: mutant R135Q and double mutants E134A,R135A and E134R,R135E all failed to achieve detectable transducin activation (Sakmar et al., 1989); in a separate study, double mutant E134R,R135E was found neither to bind nor to activate transducin (Franke et al., 1990). Given that in the present study all three mutants in which Arg-135 was replaced showed a large shift toward M II, we suggest that in wild-type rhodopsin Arg-135 plays two independent roles in the activation process—it acts to favor the M I conformation, and, within the M II structure, it contributes to the binding interaction with transducin. The conservation of Glu or Asp and Arg in the homologous positions in nearly all G-protein-coupled receptors (Probst et al., 1992) raises the possibility that this pair of charged residues may play a general role in the energetics of agonist-dependent conformational changes.

ACKNOWLEDGMENT

We thank Carol Davenport for technical assistance.

REFERENCES

Bennet, N. (1980) *Eur. J. Biochem. 111*, 99–103.
Bennett, N., Michel-Villaz, M., Kuhn, H. (1982) *Eur. J. Biochem. 127*, 96–103.
Birge, R. R., Murray, L. P., Pierce, B. M., Akita, H., Balogh-Nair, V., Findsen, L. A., & Nakanishi, K. (1985) *Proc. Natl. Acad. Sci. U.S.A. 82*, 4117–4121.
Doukas, A. G., Aton, B., Callender, R. H. & Ebrey, T. G. (1978) *Biochemistry, 17*, 2432–2435.
Emeis, D., Kuhn, H., Reichert, J., & Hofmann, K. P. (1982) *FEBS Lett. 143*, 29–34.
Franke, R. R., Konig, B., Sakmar, T. P., Khorana, H. G. & Hofmann, K. P. (1990) *Science 250*, 123–125.
Hofmann, K. P. (1986) *Photochem. Photobiophys. 13*, 309–327.
Kibelbek, J., Mitchell, D. C., Beach, J. M., & Littman, B. L. (1991) *Biochemistry 30*, 6761–6768.
Konig, B., McDowell, J. H., Kahlert, M., Hargrave, P. A., & Hofmann, K. P. (1989) *Proc. Natl. Acad. Sci. U.S.A. 86*, 6878–6882.
Kuhn, H., Mommertz, O., & Hargrave, P. A. (1982) *Biochim. Biophys. Acta 679*, 95–100.
Lamola, A. A., Yamane, T., & Zipp, E. (1974) *Exp. Eye Res. 18*, 19–27.
Longstaff, C., Calhoun, R. D., & Rando, R. R. (1986) *Proc. Natl. Acad. Sci. U.S.A. 83*, 4209–4213.
Mathews, R. G., Hubbard, R., Brown, P. K., & Wald, G. (1963) *J. Gen. Physiol. 47*, 215–240.
Nakayama, T. A., & Khorana, H. G. (1991) *J. Biol. Chem. 266*, 4269–4275.
Nathans, J. (1990a) *Biochemistry 29*, 937–942.
Nathans, J. (1990b) *Biochemistry 29*, 9746–9752.
Oprian, D. D. (1992) *J. Bioenerg. Biomembr. 24*, 211–217.
Papermaster, D. S., & Dreyer, W. J. (1974) *Biochemistry 13*, 2348–2444.
Probst, W. C., Snyder, L. A., Schuster, D. I., Brosius, J., & Sealfon, S. S. (1992) *DNA Cell Biol. 11*, 1–20.
Radding, C. R. & Wald, G. (1956) *J. Gen. Physiol. 30*, 909–923.
Robinson, P. R., Cohen, G. B., Zhukovsky, E. A., & Oprian, D. D. (1992) *Neuron 9*, 719–725.
Sakmar, T. P., Franke, R. F., & Khorana, H. G. (1989) *Proc. Natl. Acad. Sci. U.S.A. 86*, 8309–8913.
Schertler, G. F. X., Villa, C., & Henderson R. (1993) *Nature 362*, 770–772.
Weitz, C. J., & Nathans, J. (1992) *Neuron 8*, 465–472.
Yoshizawa, T., & Shichida, Y. (1982) *Methods Enzymol. 81*, 333–354.
Zhukovsky, E. A., & Oprian, D. D. (1989) *Science 246*, 928–930.